Taylor & Francis
Taylor & Francis Group

Xenobiotica
the fate of foreign compounds in biological systems

ISSN: 0049-8254 (Print) 1366-5928 (Online) Journal homepage: https://www.tandfonline.com/loi/ixen20

Disposition of asciminib, a potent BCR-ABL1 tyrosine kinase inhibitor, in healthy male subjects

Phi Tran, Imad Hanna, Fabian Kurt Eggimann, Joseph Schoepfer, Tapan Ray, Bing Zhu, Lai Wang, Petra Priess, Xianbin Tian, Florence Hourcade-Potelleret & Heidi J. Einolf

To cite this article: Phi Tran, Imad Hanna, Fabian Kurt Eggimann, Joseph Schoepfer, Tapan Ray, Bing Zhu, Lai Wang, Petra Priess, Xianbin Tian, Florence Hourcade-Potelleret & Heidi J. Einolf (2019): Disposition of asciminib, a potent BCR-ABL1 tyrosine kinase inhibitor, in healthy male subjects, Xenobiotica, DOI: 10.1080/00498254.2019.1594449

To link to this article: https://doi.org/10.1080/00498254.2019.1594449

Accepted author version posted online: 22 Apr 2019.

Disposition of asciminib, a potent BCR-ABL1 tyrosine kinase inhibitor, in healthy male subjects

Phi Tran[1], Imad Hanna[1], Fabian Kurt Eggimann[2], Joseph Schoepfer[2], Tapan Ray[1], Bing Zhu[1], Lai Wang[1], Petra Priess[2], Xianbin Tian[1], Florence Hourcade-Potelleret[2], Heidi J. Einolf[1]

[1] Novartis Pharmaceuticals Corporation, East Hanover, NJ, USA.

[2] Novartis Pharma AG, Basel, Switzerland

Corresponding Author: Phi Tran, Department of Pharmacokinetics and Sciences, Novartis Institutes for Biomedical Research, One Health Plaza, East Hanover, New Jersey, 07936, USA; phone: +1 862-778-3428; email: phi.tran@novartis.com

Abstract

1. Asciminib is a potent, specific BCR-ABL1 inhibitor being developed for the treatment of patients with chronic myelogenous leukemia (CML) and Philadelphia chromosome positive acute lymphoblastic leukemia (Ph+ ALL).
2. Here we present the results of human oral absorption, distribution, metabolism, excretion (ADME) and *in vitro* studies that together provide an overall understanding of the metabolism, distribution, and clearance of asciminib in humans.
3. Asciminib was rapidly absorbed with a maximum plasma concentration at 2 hours post-dose. Total radioactivity and asciminib showed similar terminal half-lives in plasma.
4. Oral asciminib absorption ranged between a minimum of 33%, and a maximum of 57% based on the metabolite profiles of late time-point feces collections.
5. Asciminib was eliminated mainly through feces *via* unchanged asciminib excretion and metabolism.
6. Direct glucuronidation and oxidation were major metabolic pathways in human that were catalyzed predominantly by UDP-glucuronosyltransferase (UGT)2B7 and cytochrome P450 (CYP)3A4, respectively.
7. The relative contribution of the glucuronidation pathway to the total clearance of asciminib via metabolism is estimated to range ~28-58%, whereas the relative contribution of the oxidative pathway is estimated to range ~37-64%, based upon the maximum oral absorption in humans.

Key words

asciminib, CML, BCR-ABL1 inhibitor, tyrosine kinase inhibitor, AME, UGT, glucuronide, cytochrome P450, CYP

Introduction

Chronic myeloid leukemia (CML) and the Philadelphia-positive (Ph+) subset of acute lymphoblastic leukemia (ALL) are characterized by the presence of a reciprocal translocation between chromosomes 9 and 22, leading to the generation of the BCR-ABL1 fusion protein. When fused to BCR, the tyrosine kinase activity of ABL1 becomes constitutively activated, leading to the aberrant activation of numerous downstream signaling pathways that converge to promote the growth and survival of the cell (Faderl et al., 1999).

Asciminib is a BCR-ABL1 inhibitor which differs from other currently available tyrosine kinase inhibitors (TKIs) such as bosutinib (Bosulif®), dasatinib (Sprycel®), imatinib (Gleevec®), nilotinib (Tasigna®), and ponatinib (Iclusig®) in that it is not an ATP-competitive inhibitor of BCR-ABL1. Asciminib was designed to inhibit BCR-ABL1 by targeting a distinct and separate allosteric site within the kinase domain (myristate-binding pocket) from that in which ATP-competitive TKIs bind(Adrian et al., 2006, Schoepfer et al., 2018). Asciminib mimics the myristate group to lock BCR-ABL1 in an inactive conformation and thereby inhibit the kinase activity (Skora et al., 2013, Wylie et

al., 2014). By virtue of its potent BCR-ABL1 tyrosine kinase inhibitory activity, asciminib has potential for the treatment CML and Ph+ALL patients. Furthermore, asciminib when administered in combination with an ATP-site inhibitor, has the potential to prevent the emergence of resistance due to point mutations being acquired in one of the binding sites (Wylie et al., 2014).

Asciminib is undergoing evaluation in a first-in-human (FIH) phase I clinical study as monotherapy and in combination with imatinib, nilotinib, or dasatinib for the treatment of patients with refractory CML or Ph+ ALL (study CABL001X2101). The drug has been shown to be well tolerated with the most common reported adverse events (AEs) (all grades) as headache, fatigue and increased lipase. In the same study asciminib has demonstrated anti-tumor activity at doses greater or equal to 10 mg twice daily (BID) (Novartis data on file). Based on the available preclinical and clinical data, the overall benefit-risk ratio for asciminib supports development of asciminib for patients with CML and Ph+ ALL. The effects of asciminib are currently being assessed in a phase 3 pivotal study as a single agent in patients with CML in chronic phase (CML-CP), previously treated with 2 or more TKIs (study NCT03106779). In parallel, asciminib is being evaluated in combination with imatinib in patients with CML-CP who have been previously treated with imatinib and have not achieved deep molecular response (study NCT03578367). We report here the results from a study that evaluated the absorption, distribution, metabolism and excretion (ADME) of [^{14}C]-asciminib in healthy male subjects after a single oral dose of 80 mg. The primary objectives of the study were (1) to determine the routes of excretion and mass balance of total radioactivity of [^{14}C]-asciminib in urine and feces. (2) To determine the pharmacokinetics of asciminib and

total radioactivity in blood/plasma. (3) To identify and quantify the metabolites of asciminib in plasma, urine and feces. (4) To estimate the absorption of asciminib from the urinary and fecal excretion profiles. (5) To elucidate key biotransformation pathways and clearance mechanism of asciminib in humans. Additional *in vitro* experiments were conducted to identify and characterize the enzymes [cytochrome P450 (P450s) and UDP glucuronosyltransferases (UGTs)] involved in the metabolism of asciminib. These studies were also followed up with *in vitro* studies to estimate the relative contributions of glucuronidation and oxidative metabolism pathways to overall biotransformation of asciminib. Furthermore, metabolism/transport studies examined the potential for asciminib and its primary glucuronide metabolite to undergo active biliary transport in the human hepatocyte co-culture model. The results from this human ADME study, together with results from the *in vitro* studies, provide a better understanding of the clearance mechanisms of asciminib and provide valuable information about any potential drug-drug interactions that may need to be considered when co-administering with other drugs.

Materials and Methods

Study drug: [^{14}C]-Asciminib; specific activity 1 μCi/mg, radiochemical purity ≥98%) was synthesized by the Isotope Laboratory of Novartis Pharmaceuticals Corporation (East Hanover, USA). The synthesis scheme for [^{14}C]-asciminib is provided in Supplemental information. Metabolite standards for M10, M27.5, M29.5, M30.5, M37, M43.3, and [$^{2}H_5$]-asciminib, used as internal standard for the analysis of unchanged asciminib, were synthesized by Novartis Pharmaceuticals Corporation. The preparation of the asciminib and its metabolite standards is provided in Supplemental information, or described in a patent submitted by Dodd et al (WO 2013171639). The chemical structures of radiolabeled asciminib, the position of the radiolabel along with related compounds are shown in Figure 1.

Human studies: The study protocol and the informed consent document were approved by an independent institutional review board. The written informed consent was obtained from the subjects before enrollment.

Four healthy male subjects from 19 to 29 years of age, with weights ranging from 72.8-83.4 kg, participated in the study. Subjects were housed in the study center for at least 24 hours (h) before administration of study drug and 168 h (7 days) post-dose. After an overnight fast of at least 10 h, the subjects were given a single oral dose of 80 mg of [^{14}C]-asciminib formulated as a suspension in water. To ensure the complete dosing, 80 mL of water was added to the bottle containing [^{14}C]-asciminib to suspend all of the powder in the bottle followed by three subsequent 50, 50, and 60 mL of water rinses (for a total of 240 mL). The rinsed volumes were also administered to the same subject. After the dose administration, the empty bottle was rinsed with organic solvent and the

remaining radioactivity was counted to verify the dose of [^{14}C]-asciminib given to the healthy subjects. The radioactive dose given per subject was 80 μCi based on dosimetry assessments and approved by the radiation safety committee. After administration, the volunteers continued to abstain from food for an additional 4 h.

For the quantitation of asciminib in plasma, blood was collected pre-dose and at 0.5, 1, 2, 3, 4, 6, 8, 12, 24, 36, 48, 72, 96, 120, 144, and 168 h post-dose by an indwelling cannula inserted in a forearm vein. Venous blood was collected at each time point into a K_2-EDTA containing heparinized tubes. Plasma was separated from whole blood by centrifugation, transferred to a screw-top polypropylene tube, and immediately frozen. For the determination of radioactivity in blood and plasma and for metabolite profiling, blood was collected for analysis at the same time points out to 168 h post-dose. Urine and faecal samples were collected until the majority of radioactivity was recovered up to a maximum period of 14 days post-dose. Subjects were discharged when either total recovery was ≥ 90% or if the combined urinary and fecal excretion in the preceding 48-hour period is ≤1%.

Radioactivity analysis of blood, plasma, urine, and feces samples: Analysis of total radioactivity data in plasma, blood, feces, and urine was performed by Covance Laboratories Inc., Madison, WI. All sample combustions were performed in a Model 307 Sample Oxidizer (Packard Instrument Company, Downers Grove, IL) and the resulting [^{14}C]-CO_2 was trapped in a mixture of Perma Fluor and Carbo Sorb (PerkinElmer, Downers Grove, IL). All samples were analyzed for radioactivity in Model 2900TR liquid scintillation counters (Packard Instrument Company). Plasma and urine were mixed with Ultima Gold XR (PerkinElmer, Downers Grove, IL) scintillation cocktail and

counted directly. Whole blood and fecal samples were combusted prior to liquid scintillation counting.

Safety assessments

The safety assessments included the monitoring and recording of all adverse events (AEs), serious adverse events (SAEs), laboratory tests (hematology, blood chemistry and urinalysis), vital signs, ECG, cardiac monitoring (telemetry) and physical examination.

Analysis of unchanged asciminib

A previously validated liquid chromatography tandem mass-spectrometry (LC-MS/MS) assay was slightly modified and used for the analysis of unchanged asciminib in plasma (Menssen et al 2018). The method consists of protein precipitation, evaporation of the resulting supernatant to dryness and analysis of the reconstituted sample residue by LC-MS/MS in multiple reaction monitoring (MRM) mode using ESI as the ionization technique. The method is suitable for the determination of asciminib in human plasma (K_2-EDTA) over the range of 1.00 (lower limit of quantitation, LLOQ) to 5000 ng/mL using 25.0 µL of human plasma. Briefly, plasma protein precipitation was performed in a 96-well plate. A 25 µL aliquot of the internal standard (IS) working solution was added to wells containing 25 µL of plasma. This was followed by vortex-mixing. A 200 µL aliquot of acetonitrile was added to each well to precipitate the plasma protein. The 96-well was then sealed, vortex-mixed, and centrifuged (1000 × *g*, 5 min, at room temperature). The supernatant was evaporated to dryness under nitrogen at 45^{o}C. The sample residues were reconstituted in 400 µL of 0.1% formic acid in 20% acetonitrile. For analysis, aliquots (20 µL) of the extracts were injected onto the high-performance liquid chromatography (HPLC) system.

The HPLC system consisted of a Shimadzu model LC-300AD pumps and Shimadzu model SIL-30ACMP autosampler. The column was a Mac-Mod ACE5 C8 (50 x 2.1 mm, 5µm) maintained at 35^{o}C. A gradient elution was used with flow rate set at 0.4 mL/min. The mobile phase consisted of 0.1% formic acid in water (solvent A) and 0.1% formic acid in acetonitrile (solvent B). The mobile phase was initially composed of solvent A/solvent B (80:20) and held for 0.5 min; the gradient was then linearly programmed to solvent A/solvent B (20:80) over 2 min and held for 0.5 min; back to original condition over 0.1 min; the column was equilibrated for 0.9 min; total run time was 4 min. The HPLC system was interfaced to a Sciex QTrap 6500 mass spectrometer (Applied Biosystems/MDS Sciex, Concord, ON, Canada) that was operated in the positive ion electrospray ionization mode. For multiple reaction monitoring, the transitions monitored were *m/z* 450 → *m/z* 239 for asciminib, *m/z* 455 → *m/z* 244 for the IS ([$^{2}H_5$] asciminib),). MS source temperature: 550^{o}C; dwell time: 250 msec; collision energy: 47eV.

Pharmacokinetic analyses: The following pharmacokinetic parameters were determined by non-compartmental analysis (Phoenix WinNonlin 6.3, Pharsight, Mountain View, CA): area under the blood/plasma drug concentration-time curve between time 0 and time last (AUC_{last}); AUC until time infinity ($AUC_{0-\infty}$); highest observed blood/plasma drug concentration (C_{max}); time to highest observed drug concentration (t_{max}); apparent terminal half-life ($t_{1/2}$); apparent volume of distribution of unchanged asciminib (V_z/F) calculated as Dose/(AUC • λ_z), where F is the oral bioavailability and λ_z is the terminal rate constant; and the apparent oral clearance (CL/F) was calculated as Dose/$AUC_{0-\infty}$.

Sample preparation of plasma, urine, and feces for metabolite investigation. Semi-quantitative determination of main and trace metabolites was performed by radio-HPLC with off-line microplate solid scintillation counting and structural characterization by LC-MS.

Plasma samples from each subject per time point were protein precipitated with 2 equivalent volumes of acetonitrile:ethanol: acetic acid (90:10:0.1 v/v) and removed by centrifugation. Recoveries of radioactivity averaged 89%. The supernatant was evaporated to near dryness under a stream of nitrogen using the Zymark turbo-vap LV (Zymark Corp., Hopkinton, MA), and the residues were reconstituted in 110 μL of methanol: water: formic acid (50:50:0.1, v/v) and 45 μL were injected onto the HPLC system with off-line radioactivity detection. Urine was pooled from 0 to 48 h, accounting for >90% of the dose recovered in urine and was proportional to the volume of urine collected at each time point. An aliquot of the pooled urine was concentrated approximately 8-fold by reducing the sample volume under a gentle stream of nitrogen then combined with 50 μL methanol: water: formic acid (50:50:0.1; v/v) followed by centrifugation at 3500 rpm for 10 min. The aliquot was then injected onto the HPLC system with off-line radioactivity detection. Feces homogenates were pooled (from 0 to 96 h or 0-168 h) on a weight basis to account for >90% of the dose recovered in feces. Each pooled fecal samples was extracted three times with acetonitrile; by vortex-mixing and centrifugation. The average recovery of sample radioactivity in the organic extracts was 95%. Aliquots of the combined supernatant were evaporated to dryness under nitrogen, reconstituted in methanol: water: formic acid (50:50:0.1, v/v), and aliquots

(45 µL) of the concentrated, reconstituted samples were injected onto the HPLC system with off-line radioactivity detection.

HPLC instrumentation for metabolite pattern analysis. Asciminib and its metabolites in plasma and excreta were analyzed by ultra-performance liquid chromatography (UPLC) with off-line radioactivity detection using a Waters Acquity UPLC system (Waters, Milford, MA), equipped with a Phenomenex Gemini C_{18} column (3 µm, 4.6 × 150 mm) and a guard column of the same phase, both maintained at a temperature of 30°C. Asciminib and its metabolites were resolved with gradient elution consisting of 4 mM ammonium acetate containing 0.15% formic acid (v/v) (solvent A) and acetonitrile (solvent B), at a flow rate of 1 mL/min. The gradient elution program was as follows (all step were linear): 0-2 min, 3% solvent B; 2-10 min, 25% solvent B; 10-39 min, 25-34% solvent B; 39-42 min, 34-44% solvent B; 42-45 min, 44-95% solvent B, hold at 95% solvent B for 5 min. The mobile phase condition was returned to the starting solvent mixture over 0.5 min. Then system was allowed to equilibrate for 10 min prior to the next injection.

The UPLC eluent was fractionated into a 96 deep-well Lumaplate™ (Packard Instrument Company) microplates using a Collect Pal fraction collector (Leap Technologies, Carrboro, NC) with a collection time of 7.5 sec per well. Samples were dried under a stream of nitrogen, sealed, and counted for 15–40 min per well on a TopCount® microplate scintillation counter (Packard Instrument Company).

The amounts of unchanged asciminib and metabolites in plasma or excreta were derived from the radio-chromatograms (metabolite patterns) by dividing the radioactivity in original sample in proportion to the relative peak areas. Unchanged asciminib or

metabolites were expressed as concentrations (ngEq/mL (ngEquivalent/mL)) in plasma or as percentage of dose in excreta. These values are to be considered as semi-quantitative only, as opposed to that determined for the unchanged asciminib using the validated quantitative LC/MS/MS assay.

Structural characterization of metabolites by LC-MS/MS.

Metabolite characterization was conducted with a Waters two-channel Z-spray (LockSpray^{TM}) time-of-flight mass spectrometer (Synapt MS, Manchester, UK). Leucine enkephalin was used as the mass reference standard for exact mass measurement and was delivered *v*ia the second spray channel at a flow rate of 10 µL/min. The eluent from the HPLC column was split, and about 200 µL/min was introduced into the atmospheric ionization source after diverting to waste during the first 4 min of each run to protect the mass spectrometer from nonvolatile salts. The mass spectrometer was operated at a resolution of ~10000 m/Δm_{FWHM} with spectra being collected from 100 to 1000 amu. The ionization technique employed was positive electrospray. The sprayer voltage was kept at at 3100 V and the sampling cone voltage was kept at a potential of 20 V. For the TOF MS/MS experiments, trap energies of 25 to 45 eV and transfer energy of 15 eV were used with argon as the collision gas.

***In vitro* experiments**

Kinetic analysis of asciminib metabolism by human liver microsomes.

The kinetics of [^{14}C]-asciminib metabolism (specific activity of 53.2 mCi/mmol and radiochemical purity 99%) was evaluated using pooled human liver microsomes (HLM, n = 150 donors, mixed gender; Corning, Gentest, Woburn, Massachusetts) in the presence of NADPH or UDPGA. HLM (1.5 mg protein/mL) in 100 mM potassium phosphate

buffer (pH 7.4) was preincubated with alamethicin (60 μg alamethicin/mg protein, final concentration) for 15 min on ice (for glucuronidation reactions only). $MgCl_2$ (5 mM, final concentration) was added as well as various concentrations of [^{14}C]asciminib (0.5% DMSO v/v, final concentration). The samples were thermally equilibrated for 3 min at 37°C and were initiated by the addition of the cofactor (1 mM ß-NADPH or 4 mM UDPGA, final concentration). The duplicate samples were incubated for 30 min at 37°C. The samples were quenched with half volume of cold acetonitrile and the precipitated protein was removed by centrifugation at 39,000 × *g* for 10 min at ~4°C in an Avante 30 high speed microcentrifuge (Beckman Coulter, Fullerton, CA). [^{14}C]-Asciminib and its metabolite(s) were analyzed by HPLC with off-line radioactivity detection, as described below. The percentage of impurity co-eluting with metabolites was accounted for in the reactions containing co-factor by subtraction of the percent impurity from the control samples (no cofactor). The percent of radiochemical impurity in these reactions was < 4%.

Metabolism of asciminib by human hepatocytes.

Primary human hepatocyte suspensions (single female donor, Triangle Research Labs, Lonza, Research Triangle Park, NC) were pelleted (100 × *g* for 10 min at 4°C) and re-suspended in Krebs-Henseleit maintenance medium (KHB) supplemented with sodium biocarbonate, fructose, and glycine (final concentrations of 25, 10, and 3 mM, respectively). The cells were pelleted as described above and re-suspended in the above medium supplemented with 2% (v/v) FBS (mKHB) to achieve a final concentration of ~2 × 10^6 cells·mL^{-1}. Five hundred microliters (~1 × 10^6 cells) of the final cell suspension was added to each well of a 12-well plate pre-dispensed with 0.5 mL of mKHB

containing [^{14}C]asciminib (2.5 μM nominal concentrations) and incubated at 37°C in a humidified cell culture incubator (5% CO_2, 95% air) without shaking. At various time points (0.25-24 h) the contents of individual wells were collected and the empty well washed with an additional 1 mL of acetonitrile, and stored at -80°C until the time of analysis. Positive metabolism control incubations using terfenadine and 7-ethoxycoumarin confirmed the metabolic activity of the hepatocyte incubations (data not shown). Acetonitrile extracts from hepatocyte samples were concentrated under a stream of N_2 to approximately one-third of their original volume. The samples were centrifuged and the supernatant was analyzed by HPLC with off-line radioactivity detection as described below.

Metabolism of asciminib by recombinant enzymes.

To identify the enzyme(s) involved in the metabolism of asciminib in humans, several recombinant CYP, flavin monooxygenase (FMO) and UGT enzymes (Corning, Gentest) were examined for asciminib metabolizing activity. Recombinant human (rh) UGT1A1, UGT1A3, UGT1A4, UGT1A6, UGT1A7, UGT1A8, UGT1A9, UGT1A10, UGT2B4, UGT2B7, UGT2B10, UGT2B15, UGT2B17, or UGT control microsomes (1 mg protein/mL, final concentration) in 100 mM potassium phosphate buffer (pH 7.4) were preincubated with alamethicin (60 μg alamethicin/mg protein, final concentration) for 15 min on ice. $MgCl_2$ (5 mM, final concentration) and [^{14}C]-asciminib (43 μM, final concentration) were then added and the samples were thermally equilibrated at 37ºC for 3 min in an Eppendorf Thermomixer prior to initiation with UDPGA (4 mM, final concentration). The samples were incubated for 30 min at 37ºC then quenched by the addition of a half volume of cold acetonitrile. The precipitated protein was removed by

centrifugation and an aliquot of each sample was analyzed by HPLC with off-line radioactivity.

Recombinant human CYP enzymes CYP1A1, CYP1A2, CYP1B1, CYP2A6, CYP2B6, CYP2C8, CYP2C9, CYP2C18, CYP2C19, CYP2D6, CYP2E1, CYP2J2, CYP3A4, CYP3A5, CYP4A11, CYP4F2, CYP4F3A, CYP4F3B, CYP4F12 (100 pmol CYP/mL), the recombinant human FMO enzymes FMO1, FMO3, or FMO5 (1 mg microsomal protein/mL), or control microsomes were incubated with [^{14}C]-asciminib and samples prepared as described above without alamethecin pretreatment and the reaction was initiated by the addition of β-NADPH (1 mM, final concentration) for the CYP reactions or by [^{14}C]-asciminib for the FMO reactions.

Kinetic analysis of asciminib metabolism by rhCYP enzymes

Kinetic parameters of asciminib metabolism by rhCYP enzymes, CYP2C8, CYP2D6, CYP3A4, CYP2J2 and CYP4F12 were determined to estimate the relative contribution of these enzymes to the total oxidative metabolism of asciminib in human liver. Recombinant human CYP2C8 (200 pmol CYP/mL; 1.6 mg microsomal protein/mL), CYP2D6 (200 pmol CYP/mL; 1.9 mg microsomal protein/mL), CYP3A4 (150 pmol CYP/mL; 0.81 mg microsomal protein/mL), CYP2J2 (100 pmol CYP/mL; 1.4 mg microsomal protein/mL), CYP4F12 (200 pmol CYP/mL; 0.50 mg microsomal protein/mL) were thermally equilibrated with varying concentrations of [^{14}C]-asciminib (in duplicate) in 100 mM potassium phosphate buffer (pH 7.4) containing 5 mM $MgCl_2$, final concentrations, for 3 min at 37°C in an Eppendorf Thermomixer. The reactions were initiated by the addition of 1 mM NADPH (final concentration) and were incubated for 30 min at 37°C. The reactions were quenched by the addition of a half volume of cold

acetonitrile and the precipitated protein was removed by centrifugation at 39,000 × *g* for 10 min at ~4°C in an Avante 30 high speed microcentrifuge (Beckman Coulter, Fullerton, CA). An aliquot (50 µL) of the supernatant from each sample was analyzed by UPLC with off-line radioactivity detection. The percentage of impurity co-eluting with metabolites was accounted for in the reactions containing NADPH by subtraction of the percent impurity from the control samples (no NADPH). [^{14}C]-Asciminib metabolism activity was plotted against substrate concentration and the kinetic parameters, K_m and V_{max} values, were determined by non-linear regression analysis using a hyperbolic function $v = V_{max} \cdot [S]/(K_m+[S])$, or an equation for substrate inhibition (uncompetitive): $v = V_{max}/(1+K_m/[S]+[S]/K_i)$ (for certain metabolite(s) formed by rhCYP2C8 or rhCYP3A4). The K_m values were corrected for microsomal protein binding of asciminib in the *in vitro* incubation. The fraction of unbound asciminib in the microsomal incubations (fu_{mic}) was determined by ultracentrifugation (Supplemental Information and Supplemental Figure 1).

Disposition following heptocyte co-culture incubations

The disposition of [^{14}C]-asciminib (25 µM) following 30 h incubations with human hepatocytes co-cultured with human fibroblasts (Novik et al, 2017) was investigated using a modification of the supplier's protocol (Hµrel Corporation, New Brunswick, NJ). [^{14}C]-Asciminib was incubated with hepatocyte co-cultures at 37ºC in 24-well plates in a volume of ~400 µL in a tissue culture incubator without shaking. At the end of the incubation period supernatants were collected to examine the extent of [^{14}C]-asciminib biotransformation. The attached cells were rapidly washed with HBSS buffer (2×500

µL), followed by a 5 min incubation with the same buffer (300 µL) and the supernatants collected. Finally, the attached cells were treated (5 min) with a tight-junction disrupting reagent (300 µL, Hµrel Corporation) to allow molecules trapped in hepatocyte canalicular spaces to diffuse into the media. The remaining cells were treated with 70% methanol (500 µL) and the resulting suspension was centrifuged. All samples were analyzed by LC-MS/MS and asciminib and its glucuronide conjugate in each sample quantified using a standard curve constructed using a [^{14}C]-asciminib hepatocyte incubation mixture containing both parent and the glucuronide metabolite.

HPLC with radiodetection for *in vitro* experiments

The chromatographic separation was performed on a Waters Acquity Ultra Performance LC system (Waters, Milford, MA), equipped with a Phenomenex Gemini C18 column (3 µm, 4.6 x 150 mm) and a guard column of the same phase, both maintained at a temperature of 30°C. Elution was performed with a gradient of 0.1% formic acid in 1mM ammonium acetate, pH 2.8 (mobile phase A), and acetonitrile (mobile phase B) at a flow rate of 1.0 mL/min. The gradient elution program was as follows (all step were linear): 0-2 min, 2% solvent B; 2-10 min, 25% solvent B; 10-39 min, 25-34.4% solvent B; 39-42 min, 34.4-43.4% solvent B; 42-43 min, 43.4-95% solvent B, hold at 95% solvent B for 4 min. The mobile phase condition was returned to the starting solvent mixture over 0.1 min. Then system was allowed to equilibrate for 13 min prior to the next injection. Off-line radioactivity measurement was performed with TopCount low level radioactivity detection. The UPLC eluate was collected with a fraction collector at 7 sec per fraction into Deep-well LumaPlate-96 plates (PerkinElmer Life and Analytical Sciences). The

fractions were dried with a stream of nitrogen and radioactivity was counted with a TopCount NXT Microplate Scintillation and Luminescence Counter (Packard Instrument Company) at a counting time of 10 min per well.

Data analysis

To determine the metabolism activity of [^{14}C]-asciminib in the HLM kinetic assay and human hepatocyte incubations, the percent of radioactivity of each peak in the HPLC chromatogram (parent and metabolites) were quantified (totaling 100%). The amount of individual metabolites formed in the reaction was based upon the percentage of radioactivity in the product peak with respect to the total amount of [^{14}C]-asciminib in the starting reaction. For HLM, the metabolism activity was calculated as the amount of product formed per total amount of microsomal protein in the reaction per reaction time (*i.e.* nmol metabolite formed/mg microsomal protein/h). Enzyme kinetic parameters, V_{max} and K_m, for the biotransformation by HLM and major metabolizing enzymes were calculated using GraphPad PRISM (version 6.0, San Diego, CA). The parameters V_{max} and K_m were determined using the Michaelis-Menten or substrate inhibition model. Intrinsic clearance (CL_{int}) was calculated as V_{max}/K_m.

To quantify the contribution of the different metabolic pathways to asciminib clearance in human hepatocytes, the clearance of [^{14}C]-asciminib by formation of each metabolite or pathway was determined. The intrinsic clearance by a specific metabolic pathway (e.g. CYP- or UGT-mediated) in hepatocytes ($CL_{int,hep}$, units of μL/h/10^6 cells) was calculated based on the disappearance of parent compound to the formed metabolite(s) as a function of time (measured in h) using the integrated Michaelis–Menten equation, as described by Equation 1 (Obach et al 1997).

$$CL_{int,hep} = \frac{0.693}{t_{½}} \times \frac{V}{N}$$ Eq. 1

Where $t_{½}$ is the half-life that was derived from the disappearance of parent by the formation of the specific metabolite(s) as a function of time (measured in h), ($0.693/t_{½}$) is the apparent first-order rate constant for disappearance of parent as a function of time, V is the final incubation volume (1000 µL) and N is the number of cells (in millions) per incubation. Only those data within the linear range on a plot of log concentration remaining vs. time were included to determine the disappearance rate constants (in this case was up to and including the 24-h time-point).

Results:

Dose administration: The doses administered to subjects ranged from 79.4 to 81.4 mg (mean of 80.3 mg) (77.0 to 78.9 μCi, mean value of 77.9 μCi), and were close to the target dose of 80 mg (80 μCi).

Safety and tolerability data: A single oral dose of 80 mg [^{14}C]-asciminib was generally safe and well tolerated by healthy male subjects enrolled in this study. Three subjects (75%) reported at least one AE during the study. All the AEs reported were of grade 1 severity. Headache, photophobia, blurred vision, head discomfort and dizziness were the reported AEs suspected by the investigator to be related to the study drug. There were no severe adverse events (SAEs) or other clinical relevant AEs reported in the study. No subjects discontinued from the study due to an AE. No subjects had clinically significant changes in laboratory measurements, vital signs, and ECG test results in the study

Pharmacokinetics of asciminib and total radioactivity in healthy volunteers: The mean plasma concentration-time profiles of unchanged asciminib and total radioactivity, after a single oral administration of [^{14}C]-asciminib after a dose of 80 mg are presented in Figure 2. The pharmacokinetic parameters of unchanged asciminib and total radioactivity are reported in Table 1.

Following a single oral administration of 80 mg of [^{14}C]-asciminib, the geometric mean of the peak concentration (C_{max}) of unchanged asciminib in plasma was 1790 ng/mL and T_{max} was reached at a median time of 2 h (range: 2-3 h). The geometric mean terminal $T_{1/2}$ was 14.2 h. The geometric mean systemic exposure (AUC_{inf}) was 18400 ng.h/mL, with apparent oral clearance (CL/F) of 4.34 L/h and apparent volume of distribution

(V_z/F) of 89.0 L. The inter-subject variability is low, with CV% of ~11% for both C_{max} and AUC_{inf}.

Following a single oral dose of 80 mg of [^{14}C]-asciminib, the geometric mean total radioactivity peak concentration (C_{max}) in blood was 950 ngEq/mL and T_{max} was reached at a median time of 2 h (range: 2-3 h). In plasma, the geometric mean C_{max} was 1720 ngEq/mL and T_{max} was reached at a median time of 2.5 h (range: 2-3 h). The mean blood: plasma AUC ratio for total radioactivity was 0.58, suggesting that the drug related radioactivity has a preferential distribution to plasma. The geometric mean terminal half-lives of radioactivity in blood and plasma were similar, 11.7 h and 11.6 h, respectively.

Total radioactivity and asciminib showed similar terminal half-lives in plasma (geometric mean of 11.6 and 14.2 h, respectively), indicating an approximately parallel decrease of parent compound and metabolites. This finding is consistent with asciminib being the predominant drug-related component in circulation.

Excretion and mass balance in urine and feces: After a single oral dose of 80 mg of [^{14}C]-asciminib, the excretion of radioactivity from all four subjects in urine and feces is presented in Table 2. Overall, good mass balance was achieved in all four subjects. The mean recovery of radioactivity in urine and feces was 91.0% (± 2.25% dose) over the 216 h study, with recovery in individual subjects ranging from 88.5 to 93.9%. The radioactivity was excreted predominantly in the feces, averaging 80.0% of the total dose. Renal excretion was minor, accounting for 11.0% of the total dose.

Metabolite Profiling: The metabolite profile summarizing the pharmacokinetics of asciminib and its metabolites in plasma and percentage of asciminib and its metabolites in

excreta are presented in Table 3 and Table 4, respectively. A representative HPLC radio-chromatogram of circulating metabolites is shown in Figure 3A.

In plasma, in each of the subjects, parent asciminib was the predominant drug-related component at all time points analyzed, ranging from 91.9 to 94.2% of the total radioactivity $AUC_{0\text{-}24h}$, with an average value of 92.7% (Table 3). Metabolites detected involved glucuronidation and oxidation at the pyrrolidinol ring (ketone formation, oxidative ring opening). Metabolite M30.5 (direct *O*-glucuronide of asciminib) accounted for an average of 4.93% of total AUC. Minor metabolite M44 (oxidation of alcohol to ketone) accounted for 1.88% of total AUC. Trace amount of M29.5 (alcohol formed from oxidative opening of the pyrrolidinol ring; 0.39% of total AUC) was also detected.

Representative HPLC radio-chromatograms for metabolites in urine and feces (cumulative profile) are shown in Figure 3B and Figure 3C, respectively. After the oral administration of asciminib to humans, a total of 10 radiolabeled metabolites of asciminib were characterized and quantified in the excreta. In urine, unchanged asciminib averaged 2.5% of the dose (Table 4). The mean renal clearance (CLr) for asciminib was estimated by dividing the mean amount of asciminib excreted in the urine (2.0×10^6 ng) by the mean plasma $AUC_{0\text{-}inf}$ of asciminib (18500 ng*h/mL). The estimated mean CLr of asciminib (0.108 L/h) was 1.4% of the glomerular filtration rate (7.5 L/h). The most abundant metabolite detected in the urine was M30.5 (averaged 7.0% of dose). Other metabolites included M8 (amide hydrolysis), M10 (*O*-dealkylation), M27.5 (*N*-glucuronide of asciminib), M29.5, M37 (carboxylic acid metabolite derived from oxidative opening of the pyrrolidinol ring), M39 (another carboxylic acid metabolite

derived from oxidative opening of the pyrrolidinol ring) and M43.3 (carboxylic acid metabolite). These minor metabolites were present at ≤ 0.4% of the dose (Table 4).

In the cumulative feces (pooled from 0-96 h or 0-168 h, a representative chromatogram is shown in Figure 3C), asciminib averaged 56.7% of the administered radioactive dose. The fecal profiles showed M39 and M43.3 as the most prominent metabolites, accounting for approximately 7.8% (M39) andapproximately 34.6% (M43.3) of the administered dose. Minor metabolites detected included M10, M27.5, M29.5, M37, M44 and M45. These minor metabolites were present at ≤2.2% of the dose. Metabolite M30.5 (*O*-glucuronide of asciminib) although detected in urine as the dominant component, was absent in the feces. Metabolite M30.5 (direct glucuronide), presumably, was converted back to parent asciminib while residing in the luminal tract, possibly catalyzed by glucuronidase within the gastro-intestinal tract (Aura AM et al, 2002). The absence of M30.5 in the feces was consistent with an *in vitro* study investigating the stability of metabolite M30.5 in human feces, which demonstrated near complete hydrolysis of M30.5 resulting in the formation of asciminib (data not shown). Due to the unstable nature of the glucuronide in the gastrointestinal tract, the extent to which asciminib was eliminated via metabolism to the glucuronide vs. excretion intact could not be readily assessed. Hence, the percentage of intact asciminib (56.7% of the dose) that is detected in the feces is likely to be over-estimated. Furthermore, the extent to which M30.5 contributed to the disposition of asciminib could not be easily assessed in this *in vivo* study.

The metabolite profiles were also obtained from the late time point feces (pooled from 96-144 or 144-168 h, a representative chromatogram is shown in Figure 3D). With regard to metabolites, the radiochromatograms from the cumulative feces and late feces were similar. However, asciminib was more prominent in the cumulative feces profiles, representing 68-77% of the radiochromatographic area compared to 52-55% in the late-time point feces profiles (data not shown). The late-time point profile is assumed to represent the drug-related material that has been absorbed and subsequently excreted (no unabsorbed, unchanged asciminib present). On the other hand, the cumulative profile represents a combination of drug-related material eliminated in the feces from absorbed and unabsorbed portions. These assumptions were used to estimate the maximum absorption fraction of asciminib as detailed below.

Estimation of minimum and maximum absorption fraction of asciminib

The minimum absorption was estimated using the following equation:

Minimum absorption = dose recovered in urine + dose recovered in feces as metabolites.

The mean radioactive dose recovered in the urine was 11.0% (Table 2), the mean radioactive dose recovered in the feces in the form of metabolites was 21.8% (sum of all metabolites detected in feces, Table 4). Based on these values, the estimated minimum level of oral absorption was 33%.

The maximum extent of oral absorption for asciminib in human was estimated using the late feces profiles and was based on the following assumptions: (1) The cumulative feces profile (Figure 3C) represents both absorbed and unabsorbed asciminib-related material. The absorbed portion comprised both unstable glucuronide metabolite(s) that were

converted back to parent asciminib, and asciminib which was either excreted via bile and/ or direct intestinal secretion. (2) The late time point feces profile (Figure 3D) represents asciminib-related material that has been absorbed and subsequently excreted (no unabsorbed asciminib present). Once the contribution from unabsorbed drug is subtracted out, the ratio of asciminib to metabolites is assumed to be constant over time. The absorbed asciminib-related fraction was calculated using the following equation:

Fraction asciminib absorbed = ratio of asciminib/metabolites from late feces profiles × *fraction of dose detected as metabolites in cumulative feces profiles.*

For this study, a mean ratio of asciminib/metabolites of 1.1 was obtained from the late feces profiles, and the mean fraction of dose detected as metabolites in cumulative feces profiles was 21.8%. Thus, the estimated absorbed asciminib-related fraction was 24%. A maximum absorption of approximately 57% was obtained by adding the 24% absorbed asciminib -related obtained above to the minimum estimated absorption of 33%.

Metabolite characterization by mass spectrometry: Metabolite structures were characterized by LC-MS/MS using a combination of full and product ion scanning techniques and elemental composition by exact mass measurement. The structure of major metabolites, where possible, was supported by comparisons of their chromatographic retention times and mass spectral fragmentation patterns with those of synthetic standards.

Under positive ESI, asciminib had a MH^+ ion occurred at *m/z* 450 with characteristic fragment ions observed at *m/z* 211, 239, 257, 330, 390, 404, 422 and 432 (Figure 4). Cleavage at the amide bond with charge retention on the carbonyl site generated the

fragment at *m/z* 257, subsequent loss of CO and of H_2O gave fragment at *m/z* 211. Neutral loss of H_2O from asciminib produced the major fragment at *m/z* 432, while loss of the chlorodifluoromethanol side chain plus one molecule of H_2O produced the fragment at *m/z* 330. Cleavage across the pyrrolidinol ring produced fragments at *m/z* 390, 404 and 422. High resolution mass spectral information for each of these major fragment ions supported the proposed fragmentation. Analogous fragment ions were observed in the mass spectra of the metabolites, which allowed the assignment of regions of biotransformation (Table 5).

The proposed biotransformation pathways and partial or complete structures of the metabolites are given in Figure 5.

Metabolite pathways of asciminib in human: The metabolism of asciminib involved the following primary biotransformation pathways: oxidation at the pyrrolidinol ring, direct glucuronidation, *O*-dealkylation, and amide hydrolysis (Figure 5). Oxidative opening of the pyrrolidinol ring formed the alcohol metabolite M29.5 and the carboxylic acid metabolites M37, M39 and M43.3. Together, these four metabolites accounted for approximately 17% of the dose elimination in human excreta (Table 4). Oxidation of the pyrrolidinol ring led to the formation of metabolites M44 and M45, together accounted for a total of 3.0% of dose. Direct glucuronidation pathway formed metabolites M27.5 (*N*-glucuronide of asciminib) and M30.5 (*O*-glucuronide of asciminib). Metabolite M27.5 was detected in both urine and feces (2% of dose), while M30.5 was observed in the urine but not the feces, and was the major component in the urine radiochromatogram (7% of dose). The amide hydrolysis and *O*-dealkylation pathways led to the formation of M8 and M10, respectively. Metabolite M8 accounted for 0.4% of the dose while metabolite M10

accounted for 0.8% of the dose. All metabolites detected in this human study were also observed in the rats, and/or monkeys *in vivo* (Supplemental Figure 2).

***In vitro* metabolism experiments**

Metabolite profile in HLM

[^{14}C]-Asciminib was metabolized in HLM in the presence of NADPH to form the oxidative metabolites M10, M28.5, M29.5, M32, M39, M43.3, and M44. Direct glucuronide metabolites M27.5, M30.5, and M36 were detected in HLM incubations that contained UDPGA. The metabolic pathways of [^{14}C]-asciminib in HLM is provided in Supplemental Figure 3. Metabolites M27.5 and M36 are both *N*-glucuronides of asciminib, their synthesis were given in Supplemental information. Metabolites M28.5, M32 and M36 were not detected (or below the detection limit) in human *in vivo*.

Enzyme kinetics of asciminib metabolism in HLM

Kinetic parameters (K_m, V_{max}) of [^{14}C]-asciminib metabolism in pooled HLM in the presence of NADPH or UDPGA were determined by the analysis of [^{14}C]-asciminib concentration dependence on the rate of metabolite formation and non-linear regression analysis of the steady-state data. The unbound K_m value (corrected for microsomal protein binding, see Supplemental data) for total [^{14}C]-asciminib oxidative metabolism (formation of M10, M28.5, M29.5, M32, M39, M43.3, and M44) was estimated to be 12.6 ± 0.81 μM and the V_{max} value was 1.56 ± 0.055 nmol/h/mg protein. The unbound intrinsic hepatic microsomal oxidative clearance ($CL_{int,u}$ was estimated to be 0.124 mL/h/mg protein (Table 6).

The unbound K_m value for total [^{14}C]-asciminib direct glucuronide conjugate formation (formation of M27.5, M30.5, and M36) was estimated to be 12.4 ± 1.4 μM and the V_{max}

value was 2.84 ± 0.16 nmol/h/mg protein. The unbound intrinsic hepatic microsomal conjugative clearance was estimated to be 0.229 mL/h/mg protein. Consequently, the total unbound hepatic intrinsic clearance ($CL_{int,u}$ total), which represents the sum of the oxidative and conjugative intrinsic clearances is estimated to be 0.353 mL/h/mg protein. The oxidative and glucuronidation pathways constituted ~35% and ~65% of overall clearance, respectively.

Contributions of oxidative vs. glucuronidation pathways in human hepatocytes

Direct glucuronidation was the major biotransformation pathway in human hepatocytes (consistent with the HLM CL_{int} assessment), leading to the formation of the major direct glucuronides M27.5, M30.5, and M36. The other major metabolites included the oxidation products M39 and M44. To better quantify the contribution of the different metabolic pathways to asciminib clearance in human hepatocytes, the clearance of asciminib by formation of each metabolite or pathway was determined. As shown in Supplemental Table 4, formation of each metabolite (as a percent of the total radioactivity of the integrated metabolite peaks with time) is listed with the proposed metabolic reaction and enzyme involved in its formation. The intrinsic clearance by a specific metabolic pathway (e.g. CYP-, UGT2B17-, UGT2B7-, or UGT1A3/UGT1A4-mediated) in hepatocytes was calculated based on the disappearance of parent compound to the formed metabolite(s) as a function of time as described in the Materials and Methods section. The calculated intrinsic clearance of asciminib by formation of specific metabolites in human hepatocytes can be found in Table 8. The percent contribution of CYP-mediated oxidative clearance was estimated to be 35% and the glucuronidation pathway was 60% (5% as uncharacterized P20). This result was in-line with the

contributions determined from HLM, *vide supra*. Assuming UGT2B17 contributed insignificantly to the formation of M30.5 (as mentioned above) the contribution of UGT2B17 (formation of M27.5), UGT2B7 (formation of M30.5), and UGT1A3/4 (formation of M36) to total glucuronidation clearance of asciminib in hepatocytes was estimated to be 27.9, 47.9, and 24.2%, respectively (Table 8). This higher contribution of UGT2B7 to the total glucuronidation clearance of asciminib was in-line with the chemical inhibition results (Supplemental Table 1).

Biotransformation of asciminib by recombinant human enzymes

Microsomes prepared from baculovirus-infected insect cells expressing single human CYP, UGT, and FMO enzymes were used to examine the ability of specific enzymes to metabolize [^{14}C]-asciminib. There was no metabolism of [^{14}C]-asciminib by FMO1, FMO3, or FMO5 observed in this study. The human CYP enzymes found capable of asciminib oxidative metabolism were CYP1A1, CYP1B1, CYP2C8, CYP2C9, CYP2D6, CYP2J2, CYP3A4, and CYP4F12 determined from incubations with 19 individual recombinant human CYP enzymes. Due to the lack of endogenous expression of CYP1A1 and CYP1B1 in liver and very low metabolism by recombinant CYP2C9, further evaluation of these enzymes for asciminib clearance contribution was not performed. Relative contributions of CYP2C8, CYP2D6, CYP2J2, CYP3A4, and CYP4F12 to total asciminib oxidative clearance in HLM were assessed by individual CYP enzyme kinetics using recombinant CYP enzymes and scaling of the clearance by the CYP abundance in HLM. As shown in Table 7, the relative contributions of individual CYP enzymes to asciminib hepatic oxidative clearance in HLM were 96% by CYP3A4, 2.08% by CYP2J2, 1.36% by CYP2C8, and 0.574% by CYP2D6. Due to the

very low intrinsic clearance by recombinant CYP4F12, the clearance of asciminib by this enzyme was deemed negligible.

Following incubations with 13 individual recombinant human (rh) UGT enzymes, UGT1A3, UGT1A4, UGT2B7, and UGT2B17 were found capable of asciminib direct glucuronidation. The metabolite M36 was detected in incubations with rhUGT1A3 and rhUGT1A4, whereas rhUGT2B7 formed M30.5. Recombinant human UGT2B17 catalyzed the formation of M27.5 (and M30.5 to a minor extent). Based upon the relatively low formation of M30.5 compared to M27.5 by rhUGT2B17, the contribution of UGT2B17 to M30.5 formation was deemed negligible.

Incubation with human hepatocyte co-cultures

Following the 30 h incubation with the hepatocyte co-cultures, asciminib was metabolized to generate the glucuronide metabolite in addition to multiple metabolites. The extent of conversion to the glucuronide metabolite constituted ~50% of drug-related radioactivity by HPLC-radiometric detection. The amount of asciminib and the glucuronide metabolite in the hepatocytes and those trapped in canalicular spaces between hepatocytes was estimated by LC-MS/MS detection. Under these conditions, the biliary excretion index (BEI) for asciminib and the glucuronide metabolite was estimated as the percentage of amount of the individual analyte in the canalicular space compared to that in the hepatocytes and canalicular space combined. The BEI values for asciminib and the glucuronide metabolite were ~15.0% and ~30.4% suggesting that either analyte can be subject to transport into the canalicular space in a manner similar to that of *in vivo* biliary secretion (Novik et al 2017).

Contributions of metabolic pathways in human in vivo

The minimum oral absorption (33%) was first estimated from the radioactive dose recovered in the urine and the total radioactive dose recovered in the feces as metabolites. A maximum estimate of oral absorption (57%) was obtained using the late feces profiles. As described in detail above in the estimation of maximum absorption fraction of asciminib, the estimated amount of asciminib (as 24 % of dose) excreted in feces can be assumed to be due to either conversion of a glucuronide back to parent, or absorbed asciminib that was excreted via bile and/or secreted directly into the intestinal lumen. A comparison of the relative contributions of CYP- and UGT-mediated clearances to asciminib clearance using either the assumption that asciminib excreted in the feces was unabsorbed (or actively secreted) or that 24% of the unchanged asciminib in feces was absorbed and converted from a glucuronide is shown in Table 9 (Scenario A and B columns, respectively). The assumption that 24% of the unchanged asciminib in the feces was due to conversion of a glucuronide back to parent resulted in a relative contribution of the CYP- and UGT-mediated pathways of 36.6 and 58.3%, respectively (based upon mean data). The assumption that 24% of the unchanged asciminib in the feces was due to absorbed asciminib that was excreted via bile and/or secreted directly into the intestinal lumen resulted in a relative contribution of the CYP- and UGT-mediated pathways of 63.5% and 27.6, respectively.

Discussion

This study investigated the rates and routes of excretion as well as circulating metabolites of asciminib in healthy volunteers according to regulatory guidelines to drive further clinical development of the compound. This study was performed in healthy volunteers as opposed to cancer patients to avoid confounding factors from concomitant illness and co-medications. Furthermore, cancer patients are in need of effective therapy and enrolling such patients in this study would delay potential life-saving therapy by approximately five weeks (the duration of the study including screening period). Pre-clinical and clinical information regarding the behavior and adverse effects of asciminib supported the enrollment of healthy volunteers for this study, and also as a measurement of caution, women of child bearing potential were excluded from this study.

Following a single oral dose of 80 mg of [^{14}C]-asciminib to healthy subjects, the overall mean recovery of radioactivity in the excreta was ~91% in all four subjects indicating that mass balance was achieved. The mean recovery of the administered radioactivity through the last collection interval was ~80% for feces and ~11% for urine. The percentage of the dose eliminated in the urine as unchanged asciminib was minor (mean: 2.5%), renal clearance of asciminib was only 1.4% of the glomerular filtration rate (7.5 L/h), and was therefore judged to be minimal (CLr =0.108 L/h). The mean percentage of the dose eliminated in the feces as unchanged asciminib was 56.7%. However, this percentage is likely to represent an overestimation of the extent of unchanged asciminib elimination due to the unstable nature of the glucuronide metabolite M30.5 (*vide infra*).

Asciminib was rapidly absorbed with a plasma C_{max} of 1790 ng/mL (4 µM) occurring at a median time of 2 h post dose. There was good consistency in the asciminib plasma exposures between all the subjects both in terms of Cmax (CV: 10.6%) and AUCinf (CV: 10.8%). In general, there was a trend for higher observed Cmax and AUC values in this study than those observed in patients taking the same asciminib dose (80 mg, unpublished data). The median Tmax (2 h) and geo-mean $T_{1/2}$ (14.2 h) values estimated in this study were in good agreement with the data obtained from other clinical studies (unpublished data and Menssen et al., 2018).

Circulating drug-related material was primarily associated with plasma, and parent asciminib was the predominant drug-related component, accounting for 92.7% of the plasma radioactivity (mean of the $AUC_{0\text{-}24\,h}$). During the last decade, interest in drug metabolism has increased rapidly due to discussion on the potential contribution of drug metabolites to toxicity. Within this scope, the U.S Food and Drug Administration (FDA) and the International Conference on Harmonisation (ICH) issued guidance for Metabolites in Safety Testing (MIST), recommending additional safety assessments for major metabolites (Guidance for Industry, Safety Testing of Drug Metabolites, http://www.fda.gov/downloads/Drugs/guidanceComplianceRegulatoryInformation/Guidances/ucm079266.pdf; ICH, Non-Clinical Safety Studies for the Conduct of Human Clinical Trials and Marketing Authorization for Pharmaceuticals, http://www.ema.europa.eu/ich-m3-r2-non-clinical-safety-studies-conduct-human-clinical-trials-pharmaceuticals). Major metabolites are defined by both guidelines as those with a systemic exposure >10% of the total drug-related exposure that are either identified only in human plasma or present at disproportionally higher levels in humans than in any

preclinical test species. In this study, no metabolite was detected which contributed to mean plasma radioactivity $AUC_{0\text{-}24h} \geq 10\%$, hence further tests to evaluate the safety of the metabolites are not required according to the guidelines. The circulating metabolites detected were M30.5, M44 and M29.5, which accounted for approximately 5%, 2% and 0.4% of the total plasma radioactivity, respectively. In the rat ADME study metabolite M30.5 was not found in the systemic circulation (the glucuronidation pathway is absent in rats) but it was observed in monkey plasma. The minor human plasma metabolites M29.5 and M44 were also detected in the systemic circulation in the rat and monkey ADME studies (Supplemental Table 2). The metabolism of asciminib involved the following primary biotransformation pathways: oxidation at the pyrrolidine ring, direct glucuronidation, *O*-dealkylation, and amide hydrolysis. Oxidative opening of the pyrrolidine ring, a major biotransformation pathway which led to the formation of several metabolites (M29.5, M37, M39 and M43.3), accounted for approximately 17% of the dose elimination in human excreta.

The minimum oral absorption of asciminib was estimated from the radioactive dose recovered in the urine and the total radioactive dose recovered in the feces as metabolites. The minimum level of oral absorption was estimated to be 33%. In this study, ~57% of the dose was recovered as unchanged asciminib in feces. It was not easy to determine the source of unchanged asciminib in feces which can be attributed to: (1) unabsorbed asciminib, (2) absorbed, directly secreted asciminib, and (3) asciminb produced from gut microbial degradation of metabolites (mainly glucuronide metabolites), especially since no clinical intravenous PK data is available.

Using the late feces profiles, an attempt to estimate the maximum of oral absorption for asciminib was made. The estimated maximum of oral absorption for asciminib was 57%, which was in line with the absorption values reported for rats and monkey ADME studies (50-52%, Supplemental Table 3). From the late feces profiles, an absorbed asciminib-related fraction of 24% was estimated from the total % of dose detected as unchanged asciminib in the cumulative feces. The fraction (24%) of the unchanged asciminib in the feces (that was absorbed) can be assumed to be due to either (1) conversion of a glucuronide back to parent, or (2) absorbed asciminib that was excreted via bile and/or secreted directly into the intestinal lumen. In bile duct-cannulated rats dosed intravenously with 5 mg/kg [^{14}C]-asciminib, 13.1% and 22.7% of dose was excreted as parent asciminib in bile and feces, respectively (data not shown). This suggests that biliary excretion and/or intestinal secretion of unchanged asciminib may also occur to some extent in humans. Indeed, the results of the *in vitro* studies examining asciminib disposition in human hepatocyte co-cultures suggested the potential for asciminib and its glucuronide metabolite to undergo secretion into canalicular-like spaces between adjacent hepatocytes. Although the data obtained from this model is not quantitative, it represents qualitative evidence of the potential for asciminib and the glucuronide metabolite to undergo biliary secretion *in vivo*. Moreover, pre-clinical investigations have demonstrated that asciminib is substrate for P-glycoprotein (P-gp) and the breast cancer resistance protein (BCRP), which may play a role in facilitating its biliary secretion *in vivo* (data not shown).

As the magnitude of a drug interaction is sensitive to the percentage of clearance by the enzyme being inhibited (or induced), it is important to define the clearance pathways as

well as possible. Ultimately, the relative clearance pathways are defined clinically by the human radiolabeled study. Assuming that the fraction of dose estimated above (24%) was due to absorbed asciminib that was excreted via bile and/or secreted directly into the intestinal lumen, then the total % of dose excreted as asciminib unchanged would be 26.5% (24% + 2.5% asciminib excreted in urine). Metabolism (oxidative, hydrolysis and glucuronidation) accounted for another 30% of the dose (Table 4). Thus, once absorbed, asciminib would be cleared in humans via unchanged asciminib excretion and metabolism. The relative contributions of the glucuronidation and oxidative pathways to the overall metabolic clearance of asciminib would be ~27.6 and ~63.5%, respectively (Table 9, Scenario A).

In vitro investigations into the relative contribution of CYP and UGT enzymes to the overall clearance of asciminib indicated that ~35% of the observed *in vitro* intrinsic hepatic clearance of asciminb could be attributed to CYP metabolism, and ~60-65% attributed to direct glucuronidation by UGT enzymes (*i.e.* excluding pathways in which phase I oxidation occurs before glucuronidation). If it is assumed that the entire 24% of dose estimated above was due to the conversion of the unstable glucuronide M30.5 back to parent asciminib while residing in the luminal tract, then the relative contribution of the glucuronidation and oxidative pathways to the overall clearance of asciminib *via* metabolism would be approximately 58.3 and 36.6%, respectively (Table 9, Scenario B), in line with *in vitro* results. Several CYP enzymes were responsible for oxidative clearance of asciminib, with CYP3A4 being the main contributor, while UGT2B7 was responsible for the clearance of asciminib via the glucuronidation pathway. Based upon the combined *in vivo* and *in vitro* results, the relative contribution of the glucuronidation

pathway to the total clearance of asciminib via metabolism is estimated to range from ~28 - 58%, whereas the relative contribution of the oxidative pathway is estimated to range from ~37 - 64%. For asciminib, with both UGT and CYP enzymes involved in the clearance, a mechanistic clinical DDI study using a strong CYP (*e.g.* CYP3A4) inhibitor (and/or P-gp inhibitor) would be useful as well to define the contributions of these pathways.

In conclusion, a single dose administration of 80 mg [^{14}C]-asciminib was shown to be safe and well tolerated in healthy subjects enrolled in this study with no SAEs or clinically relevant AEs reported. There were no clinically significant abnormalities in laboratory evaluations, vital signs or ECG. Furthermore, the results from this study, together with the *in vitro* studies, provide a comprehensive understanding of the clearance mechanisms of asciminib and provide valuable information about any potential drug-drug interactions that may need to be considered when co-administering with other drugs.

Acknowledgements

The authors would like to thank Dr Amy Wu for providing analytical support for the radiolabeled drug substance, Dr Wenkui Li and Ms Shari Wu for supporting bioanalytical work, Dr Matthias Kittelmann and Ms Alexandra Varga for assessing the stability of asciminib glucuronide M30.5 in feces and the support in the biocatalytic reference production, Alexandre Luneau for the NMR analysis, Ms Marion Burglin for the preparation of M10, M29.5 and M37, Ms Susanne Oswald for the preparation of M43.3, Dr Mark Kagan for helpful discussion on the use of late timepoint feces metabolite profiles for the estimation of oral absorption. The in life portion of the study was conducted by Covance Clinical Research Unit Inc, Madison, WI, USA in compliance with Good Clinical Practice (GCP).

References

Achour B, Russell MR, Barber J, Rostami-Hodjegan A (2014) Simultaneous quantification of the abundance of several cytochrome P450 and uridine 5'-diphospho-glucuronosyltransferase enzymes in human liver microsomes using multiplexed targeted proteomics. Drug Metab Dispos; 42(4):500-10

Adrian FJ, Ding Q, Sim T, et al (2006). Allosteric inhibition of Bcr-abl-dependent cell profiferation. Nat Chem Biol. 2006; 2:95-102

Aura AM, O'Leary KA, Williamson G, et al (2002). Quercetin derivatives are deconjugated and converted to hydroxyphenylacetic acids but not methylated by human fecal flora *in vitro*. J Agric. Food Chem. 50(6) 1725-1730

Barter ZE, Perrett HF, Yeo KR, Allorge D, Lennard MS, and Rostami-Hodjegan A (2010) Determination of a quantitative relationship between hepatic CYP3A5*1/*3 and CYP3A4 expression for use in the prediction of metabolic clearance in virtual populations. *Biopharm Drug Dispos* 31:516–532Dodd, Stephanie Kay; Furet, Pascal; Grotzfeld, Robert Martin; Jones, Darryl Brynley; Manley, Paul; Marzinzik, Andreas; Pelle, Xavier Francois Andre; Salem, Bahaa; Schoepfer, Joseph. Preparation of benzamide derivatives for inhibiting the activity of ABL1, ABL2 and BCR-ABL1 for treating cancer. WO 2013171639

Faderl S, Talpaz M, Estrov Z, O'Brien S, Kurzrock R, Kantarjian HM (1999) The biology of chronic myeloid leukemia. New Engl J Med 341:164-172

Mano Y, Usui T, Kamimura H (2007a) Inhibitory potential of nonsteroidal anti-inflammatory drugs on UDP-glucuronosyltransferase 2B7 in human liver microsomes. Eur J Clin Pharmacol. 63(2):211-6

Mano Y, Usui T, Kamimura H (2007b) Predominant contribution of UDP-glucuronosyltransferase 2B7 in the glucuronidation of racemic flurbiprofen in the human liver. Drug Metab Dispos. 35(7):1182-7

Menssen HD, Quinlan M, Kemp C, Tian X (2018). Relative bioavailability and food effect evaluation for 2 tablet formulations of asciminib in a 2-arm, crossover, randomized, open-label study in healthy volunteers. Clin Pharmacol Drug Dev 0(0):1-10

Novik E, Dwyer J, Morelli J, Parekh A, Cho C, Pludwinski E, Shrirao A, Freedman R, MacDonald J, Jayyosi Z (2017). Long-enduring primary hepatocyte-based co-cultures improve prediction of hepatotoxicity. Toxicol Appl Pharmacol. 336:20-30.

Obach R, Baxter J, Liston T, Silber M, et al (1997) The prediction of human pharmacokinetic parameters from preclinical and *in vitro* metabolism data. J Pharmacol Exp Ther 283:46-58.

Rowland Yeo K, Rostami-Hodjegan A, Tucker GT (2004) Abundance of cytochromes P450 in human liver: a meta-analysis. Br J Clin Pharmacol. 57:687–8.

Schoepfer, Joseph; Jahnke, Wolfgang; Berellini, Giuliano; Buonamici, Silvia; Cotesta, Simona; Cowan-Jacob, Sandra W.; Dodd, Stephanie; Drueckes, Peter; Fabbro, Doriano; Gabriel, Tobias; et al. (2018) Discovery of Asciminib (ABL001), an Allosteric Inhibitor of the Tyrosine Kinase Activity of BCR-ABL1. J. Med. Chem. 61:8120-8135

Skora L, Mestan J, Fabbro D, et al (2013) NMR reveals the allosteric opening and closing of Abelson tyrosine kinase by ATP-site and myristoyl pocket inhibitors. Proc Natl Acad Sci USA. 110

Wylie A, Schoepfer J, Berellini G, et al (2014) ABL001, a Potent Allosteric Inhibitor of BCR-ABL, prevents emergence of resistance disease when administered in combination with nilotinib in an *in vivo* murine model of chronic myeolid leukemia. Blood. (124):398

Legends

Figure 1. Chemical structures of [^{14}C]-asciminib, [$^{2}H_5$]-asciminib internal standard and authentic reference standards for metabolite M10, M27.5, M29.5, M30.5, M37, and M43.3.

Figure 2. Plasma concentrations of radioactivity (squares) and asciminib (diamonds), after a single 80 mg oral dose of [^{14}C]-asciminib.

Figure 3. Representative radio-chromatograms of asciminib in plasma 3h post dose (A), urine 0-48 h (B), feces 0-96 h (C), and feces 96-144 h (D) after a single oral dose of [^{14}C]-asciminib to humans. Note that M10, M27.5, M29.5, M30.5, M37, and M43.3 were identified by retention times and CID product ion spectra that were similar to those of their synthetic standards, whereas the other metabolite structures were tentatively assigned as described under *Results*.

Figure 4. Product ion mass spectrum of asciminib

Figure 5. Metabolism of asciminib in human

Figure 1

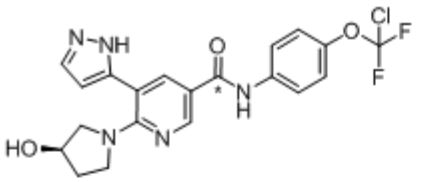

[^{14}C]-asciminib

* denotes position of radiolabeling

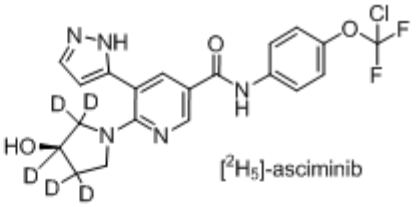

[$^{2}H_5$]-asciminib

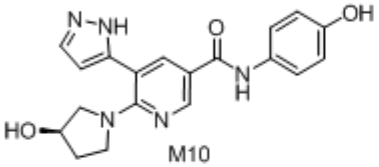

M10

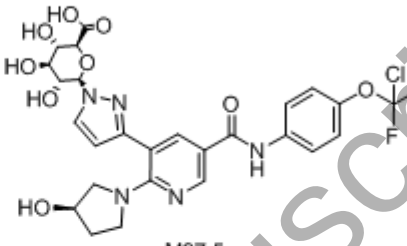

M27.5

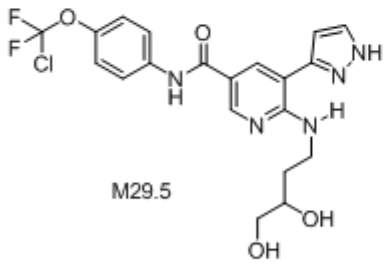

M29.5

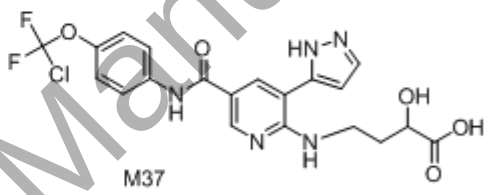

M37

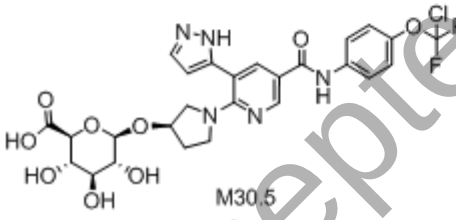

M30.5

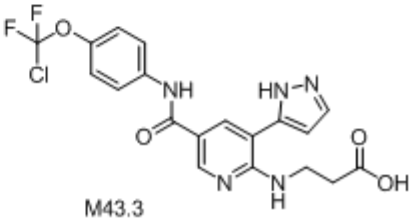

M43.3

Figure 2

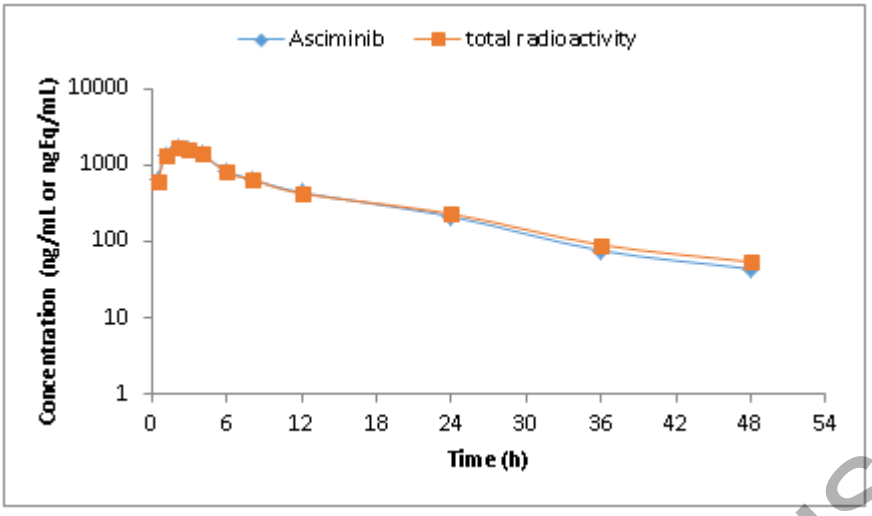

Figure 3

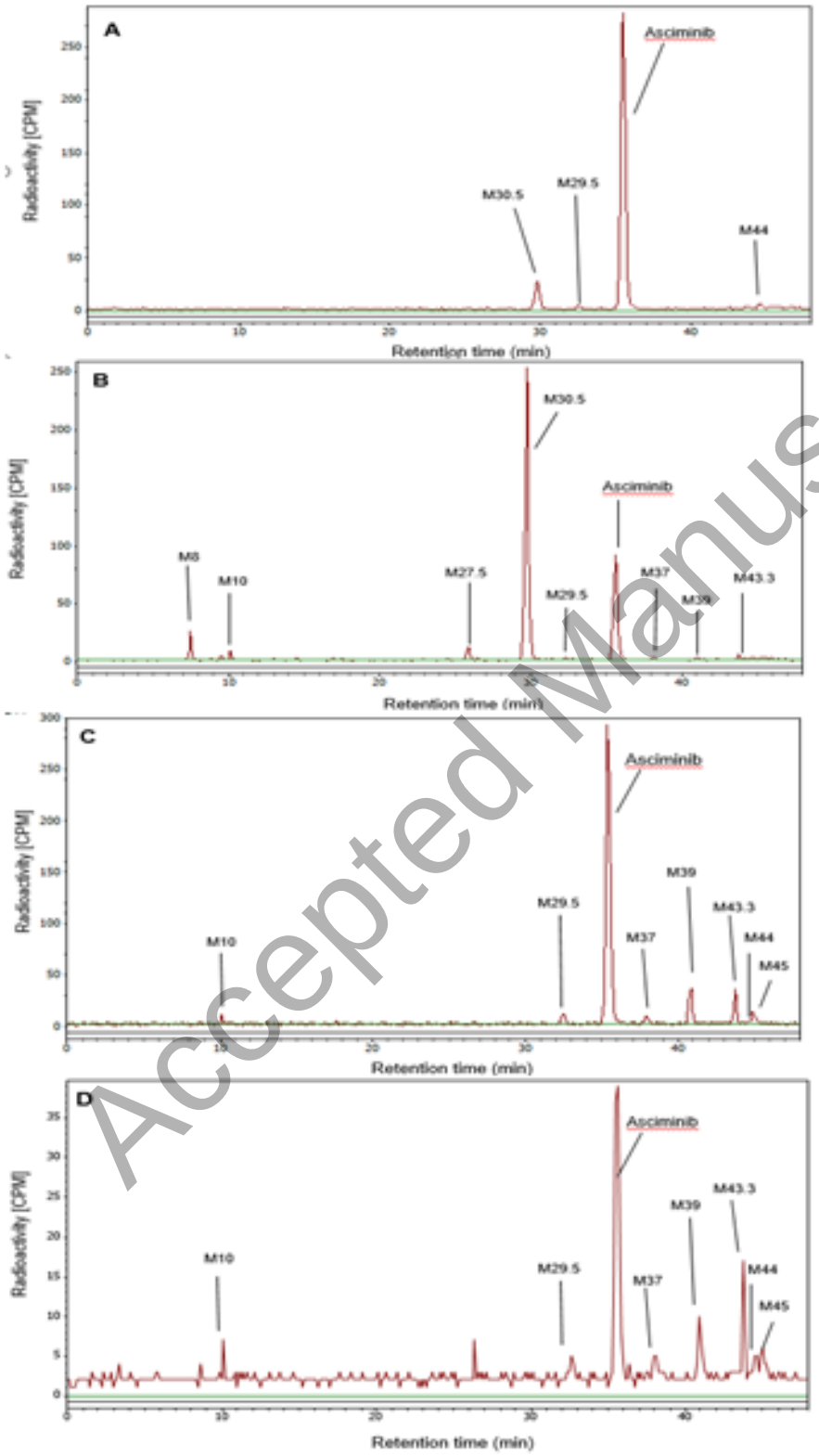

Figure 4

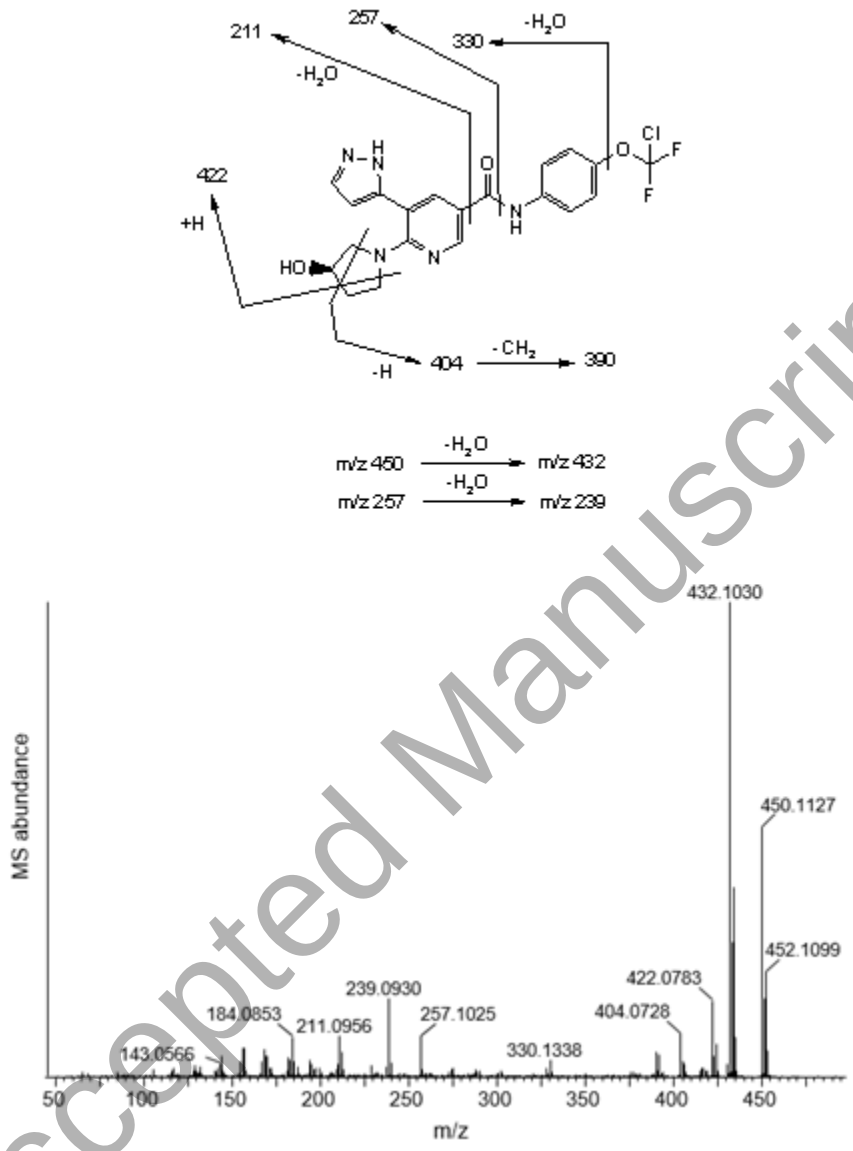

Figure 5

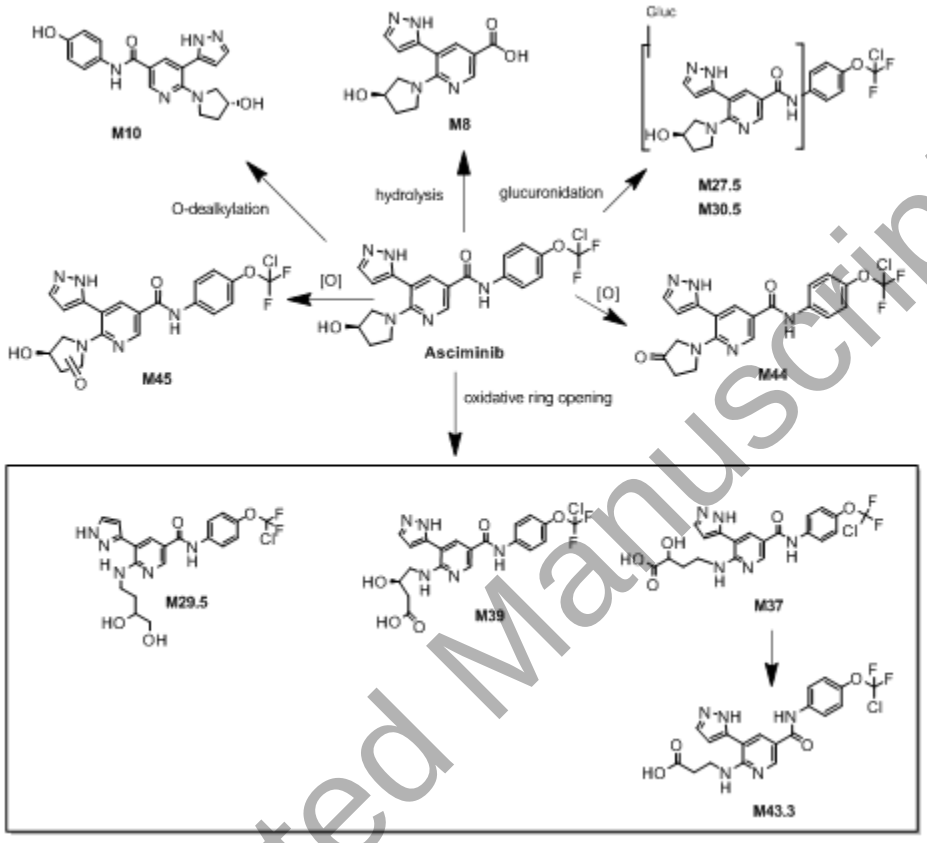

TABLE 1

PK parameters of total radioactivity in whole blood and plasma and of asciminib *in plasma (geo-mean (geo-mean CV%))*

Pharmacokinetic parameters[a]	Total radioactivity in whole blood	Total radioactivity in plasma	Asciminib in plasma
C_{max} (ng/mL) or (ngEq/mL)[a]	950 (13.5)	1720 (12.0)	1790 (10.6)
T_{max} (h)[b]	2 (2.0-3.0)	2.5 (2.0-3.0)	2 (2.0-3.0)
AUC_{last} (ngh/mL) or (ngEq•h/mL)[c]	9830 (12.2)	17600 (11.7)	18400 (10.8)
$AUC_{0-\infty}$ (ngh/mL) or (ngEq•h/mL)[c]	10600 (12.8)	18500 (12.6)	18400 (10.7)
$T_{1/2}$ (h)	11.7 (19.6)	11.6 (9.35)	14.2 (7.5)
CL/F (L/h)			4.34 (10.8)
Vz/F (L)			89.0 (6.1)

[a]ng/mL for unchanged asciminib, ngEq/mLfor total radioactivity
[b]Tmax is presented as median (range)
[c]ng*h/mL for unchanged asciminib, ngEq*h/mL for total radioactivity.

TABLE 2

Excretion of radioactivity in urine and feces following a single oral dose of 80 mg [^{14}C]-asciminib

	Percent of radioactive dose recovered by subject				
	1000-008	1000-010	1000-014	1000-016	Mean ± SD
Urine	10.1	12.5	11.8	9.37	11.0 ± 1.46
Feces	80.3	78.5	82.1	79.1	80.0 ± 1.58
Dose recovery (%)	90.5	91.0	93.9	88.5	91.0 ± 2.25

TABLE 3

Pharmacokinetic parameters of asciminib *and its metabolites in plasma after a single 80-mg oral dose of [^{14}C]-*asciminib *(mean ± SD, n=4)*

Pharmacokinetic parameters[a]	M29.5	M30.5	M44	Asciminib [b]
C_{max} (ngEq/ml)	12.1 ± 4.16	120 ± 50.0	29.0 ± 6.71	1560 ± 166
T_{max} (h)	3.8 ± 1.5	3.0 ± 0.0	2.8 ± 0.5	2.5 ± 0.6
$AUC_{0\text{-}24h}$ (ngEq•h/ml)	57.9 ± 17.2	740 ± 294	282 ± 161	13800 ± 1330
$AUC_{0\text{-}24h}$ (%)	0.39 ± 0.11	4.93 ± 1.80	1.88 ± 1.06	92.7 ± 1.03

[a]Abbreviation definitions for PK parameters are denoted in the Pharmacokinetic analysis in the Materials and Methods section.
[b]Asciminib and its metabolites were determined by HPLC with radio-detection.

TABLE 4

Amounts of asciminib *and metabolites in urine and feces following a single oral dose of 80 mg [^{14}C]-asciminib (mean % of dose ± SD; n=4)*

Metabolite	Urine [a,b]	Feces[a,c]	Total
M8	0.4 ± 0.1	nd	0.4
M10	0.1 ± 0.1	0.7 ± 0.2	0.8
M27.5	0.4 ± 0.1	1.6 ± na	2.0
M29.5	0.1 ± 0.0	1.9 ± 0.2	2.0
M30.5	7.0 ± 1.4	nd	7.0
M37	0.1 ± 0.0	2.2 ± 0.5	2.3
M39	0.1 ± 0.0	7.8 ± 1.0	7.9
M43.3	0.1 ± 0.0	4.6 ± 0.9	4.7
M44	nd	0.8 ± 0.3	0.8
M45	nd	2.2 ± 0.7	2.2
Asciminib	2.5 ± 0.5	56.7 ± 2.1	59.2

[a]Percentage of metabolite in relation to the administered dose of [^{14}C]-asciminib

[b]Sample taken from pooled urine collected 0 to 48 h post dose administration

[c]Sample taken from pooled feces collected 0 to 96 h or 0 to 168 h post dose administration

TABLE 5

Characteristic and proposed structures of asciminib metabolites

Metabolite	$[M+H]^+$	Proposed structure
Asciminib	450.1144	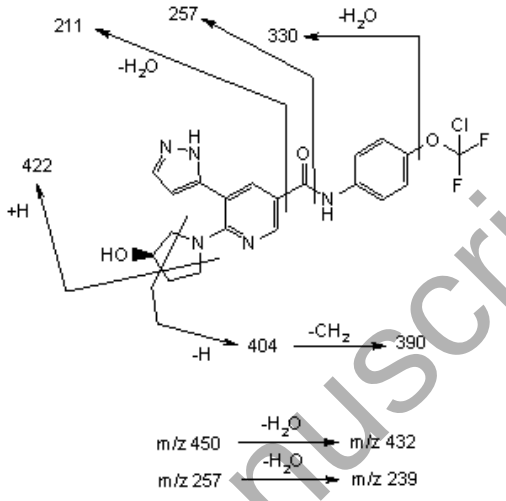
M8	273*	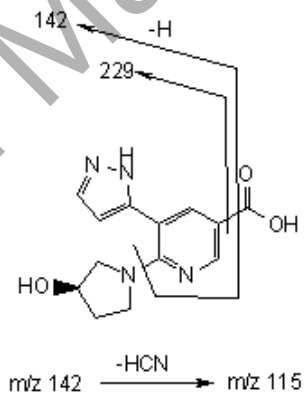

M10 366.1566

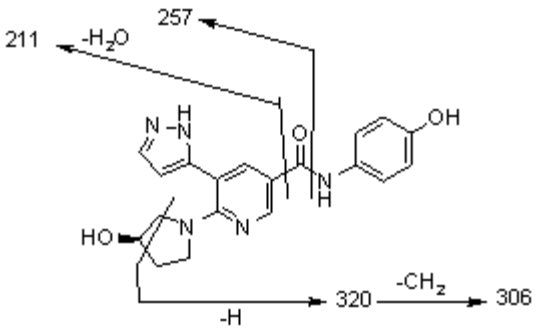

m/z 366 $\xrightarrow{-H_2O}$ m/z 348

m/z 257 $\xrightarrow{-H_2O}$ m/z 239

m/z 211 $\xrightarrow{-HCN}$ m/z 184

M27.5 626.1465

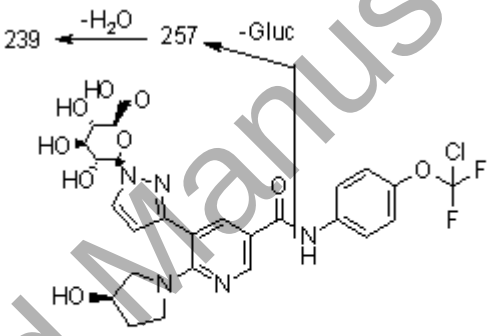

m/z 626 $\xrightarrow{-Gluc}$ m/z 450

m/z 626 $\xrightarrow[-H_2O]{-Gluc}$ m/z 432

M29.5 468.1250

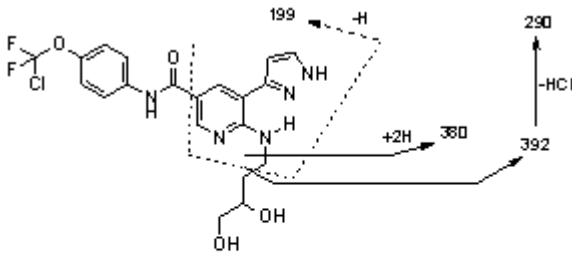

m/z 468 $\xrightarrow{-H_2O}$ m/z 450

m/z 468 $\xrightarrow{-2H_2O}$ m/z 432

m/z 199 $\xrightarrow{-CH_2,\ +2H}$ m/z 187

M30.5 626.1465

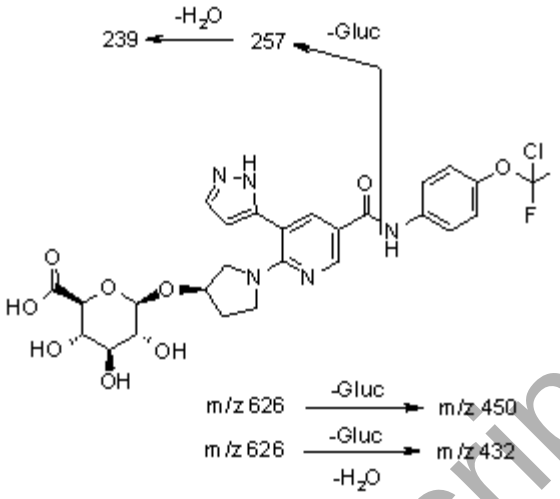

M37 482.1043

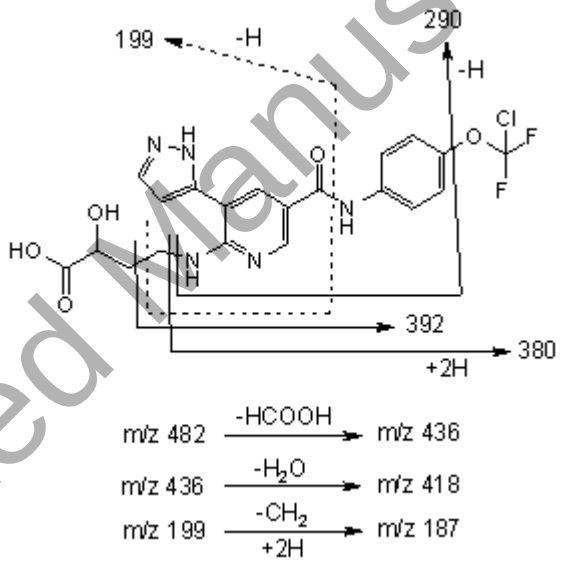

M39 482.1043

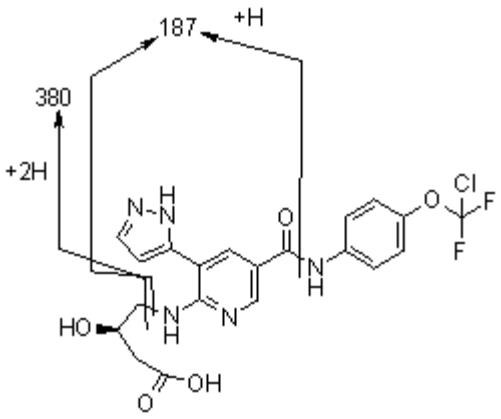

m/z 482 $\xrightarrow{-H_2O}$ m/z 464

m/z 482 $\xrightarrow{-2H_2O}$ m/z 446

m/z 464 $\xrightarrow{-HCOOH}$ m/z 418

M43.3 452.0937

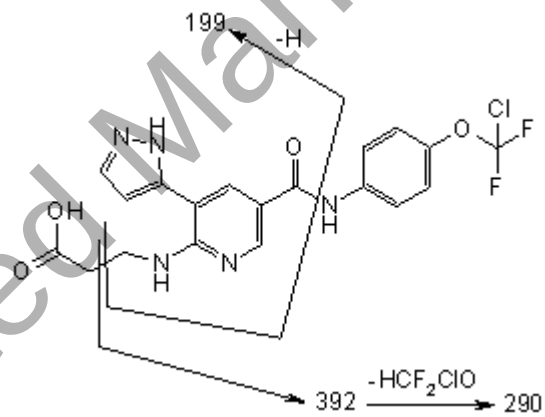

M44 448.0987

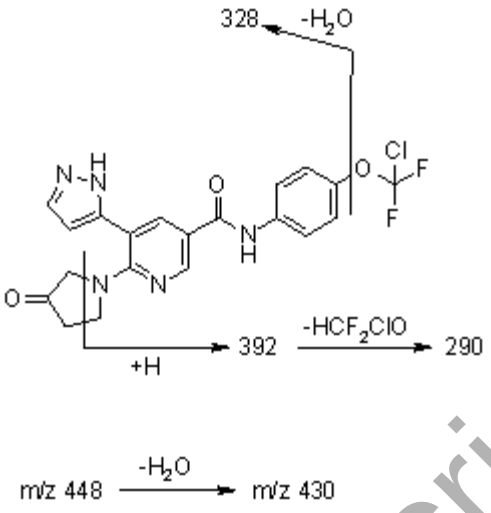

m/z 448 $\xrightarrow{-H_2O}$ m/z 430

M45 464.0937

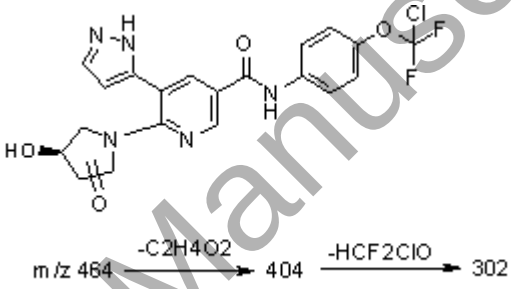

TABLE 6

Intrinsic clearance of asciminib by different metabolic pathways (oxidation vs. glucuronidation) in HLM

Enzyme/ Pathway	$K_{m,u}$[a] µM	V_{max} nmol·h^{-1}·mg protein^{-1}	$CL_{int,u}$ mL·h^{-1}·mg protein^{-1}	% contribution of pathway in HLM[b]
Oxidation[c]	12.6 ± 0.81	1.56 ± 0.055	0.124	35
Glucuronidation[d]	12.4 ± 1.4	2.84 ± 0.16	0.229	65

[a]values are the unbound K_m (K_m value* fu_{mic}); fu_{mic} for asciminib was determined to be 0.0811 for an incubation of 1.5 mg protein·mL^{-1}

[b]% contribution = oxidative or glucuronidation $CL_{int,u}/(\sum CL_{int,u\ oxidation\ and\ glucuronidation}) \times 100$

[c]Total oxidative metabolism included formation of M10, M28.5, M29.5, M32, M39, M43.3, and M44

[d]Total glucuronidation metabolism included formation of M27.5, M30.5, and M36

TABLE 7

Enzyme kinetic parameters and estimated contribution of individual CYP enzymes to the oxidative clearance of asciminib in HLM

Enzyme	$K_{m,u}$ (μM)	V_{max} (nmol/h/nmol CYP)	CL_{int} (mL/h/nmol CYP)	CYP Abundance (pmol/mg HLM)[a]	Scaled HLM $CL_{int,u}$ (mL/h/mg HLM)	Contribution (% total CYP metabolism)[d]
CYP2C8	7.60	8.85	1.16	24	0.0279	1.36
CYP2D6	30.7	45.3	1.47	8	0.0118	0.574
CYP3A4	15.7	226	14.4	137	1.97	96.0
CYP2J2	0.694	24.7	35.5	1.2	0.0427	2.08
CYP4F12	41.1	4.91	0.120	na[c]	na[c]	negligible[e]

[a]Values from Rowland Yeo et al., 2004, Barter et al., 2010, and Achour et al., 2014
[b]scaled HLM $CL_{int,u}$ = $CL_{int,u}$ x CYP abundance in HLM
[c]not available
[d]% contribution = scaled HLM $CL_{int,u}$/(sum of scaled HLM $CL_{int,u}$) x 100
[e]assumed to be negligible due to its low $CL_{int,u}$

TABLE 8

Intrinsic clearance of asciminib by different metabolic pathways/enzymes and relative contributions of individual UGT enzymes to the clearance by glucuronidation in human hepatocytes

Enzyme/ Pathway	Metabolite(s)	$CL_{int,hep}$[a] $\mu L/h/10^6$ cells	% contribution of pathway in human hepatocytes	% individual UGT contribution to total glucuronidation clearance in human hepatocytes[b]
Oxidation	M29.5, M37, M39, M44	5.352	34.84	
Glucuronidation	M27.5, M30.5, M36		60.30	
UGT2B17	*M27.5*	*2.587*	*16.84*	*27.9*
UGT2B7[c]	*M30.5*	*4.433*	*28.86*	*47.9*
UGT1A3/4	*M36*	*2.243*	*14.60*	*24.2*
uncharacterized	P20	0.7458	4.860	
TOTAL		15.36	100.0	

[a]Calculation of intrinsic clearance (CL_{int}) can be found in the Materials and Methods section and in Supplemental Table 4

[b]The relative contribution of the individual UGT enzymes were determined by normalizing each of the individual % of total CL_{int} values for UGT2B17, UGT2B7, and UGT1A3/4 by the summation of all the UGT % of total CL_{int} values ($\sum$UGT % of total CL_{int} = 16.84% (UGT2B17) + 28.86% (UGT2B7) +14.60% (UGT1A3/4) = 60%)

[c]It was assumed that UGT2B7 dominated the formation of M30.5 due to the relatively low formation of M30.5 by recombinant UGT2B17

TABLE 9

Relative contributions of enzymes/pathways to asciminib clearance in humans in vivo

Metabolite /asciminib	**Proposed reaction**	**Proposed enzyme involved**	**Average amount of parent and metabolites in excreta (expressed as % of dose)**			**Total % of dose excreted (normalized to 100%)[a] as metabolites (and asciminib in urine)**	
			urine	feces	urine + feces	**Scenario A.** Assumes unchanged asciminib in feces was unabsorbed (or actively secreted)[b]	**Scenario B.** Assumes 24% of unchanged asciminib in feces was absorbed and converted from a glucuronide[c]
M8	Hydrolysis	Unknown	0.4	-	0.4	1.23	0.707
M10	*O*-dealkylation	CYP	0.1	0.7	0.8	2.45	1.41
M27.5	Glucuronidation	UGT2B17	0.4	1.6	2	6.13	3.53
M29.5	Oxidative ring opening	CYP	0.1	1.9	2	6.13	3.53
M30.5	Glucuronidation	UGT2B7[d]	7.0	-	7	21.47	12.37
M37	Oxidative ring opening	Likely CYP	0.1	2.2	2.3	7.06	4.06
M39	Oxidative ring opening	Likely CYP	0.1	7.8	7.9	24.23	13.96
M43.3	Oxidative ring opening	CYP	0.1	4.6	4.7	14.42	8.30
M44	Oxidation	CYP	-	0.8	0.8	2.45	1.41
M45	Oxidation	Assumed CYP mediated	-	2.2	2.2	6.75	3.89
asciminib	Parent - urine		2.5	NA	2.5	7.67	4.42
asciminib	Parent-feces		NA	56.7 (33[e])	56.7 (33[e])	-	42.4[e]
TOTAL % parent + metabolites			10.8	78.5	89.3	100	100
TOTAL % Oxidation						63.5	**36.6**
TOTAL %						27.6	**58.3**

Glucuronidation		
TOTAL % Hydrolysis	1.23	**0.710**

NA, not applicable

[a]based upon the total average amount of the absorbed dose (expressed as % of dose). In scenario A. it is based upon 32.6% absorption and scenario B, 56.6% absorption

[b]The total % of dose excreted as metabolites (feces + urine) and parent in urine normalized by 32.6% (the total amount of dose excreted as metabolites in feces and the radioactive dose recovered in urine). This assumes asciminib in the feces was all unabsorbed drug (or the 24% of asciminib in feces was actively secreted)

[c]The total % of dose excreted as metabolites (feces + urine), parent in urine, plus 24% of the dose as asciminib in feces (from conversion of a glucuronide back to parent) normalized by a value of 56.6% (the total amount of dose excreted as metabolites in feces, including 24% of parent in feces, and radioactive dose recovered in urine)

[d]It was assumed that UGT2B7 dominated the formation of M30.5 due to the relatively low formation of M30.5 by recombinant UGT2B17

[e]Assumes 24% of the dose in feces arose from a glucuronide converted back to parent, based upon late fecal metabolite analysis